Using the UPFC and GUPFC Controllers to Maximize Available Transfer Capability (ATC)

Rakhmad Syafutra Lubis[1], Sasongko Pramono Hadi[2] and Tumiran[3]

[1]PhD Student in Electrical Engineering and Information Technology, Universitas Gadjah Mada, Yogyakarta, Indonesia
[2]Electrical Engineering and Information Technology, Universitas Gadjah Mada, Yogyakarta, Indonesia
[3]Electrical Engineering and Information Technology, Universitas Gadjah Mada, Yogyakarta, Indonesia

Abstract: This paper focuses on studying the effect of the unified power flow controller (UPFC) and generalized unified power flow controller (GUPFC) to maximize the Available Transfer Capability (ATC). The normalized sensitivity factors technique is used, can be approximately computed, to determine the ATC of a test system, considering a variety of system limits. The basic Voltage Stability Constrain Optimal Power Flow (VSC-OPF) solution that does not consider contingencies is used for determining the sensitivity of power flows with respect to the critical loading parameter. Then, based on this solution and assuming a small variation of the loading parameter, compute the power flows again by solving critical power flows function. Then the sensitivity of system loading factor and N-1 contingency criteria technique is used to determine an optimal location of the UPFC and GUPFC controller. Finally, using proper models of the UPFC and GUPFC controllers, the effects of this Flexible AC Transmission System (FACTS) controller on the system ATC are studied. The IEEE 57-bus and 118-bus is used as the test system for validity, computing the system ATC for a given generation and loading pattern. All realistic control limits, as well as voltage dependent loads, are used in the ATC computation, with and without FACTS controller. The GUPFC can so strong influence the system in controlling or enhancement the ATC as good as power flow possible is compared with the UPFC.

Keyword: UPFC, GUPFC. ATC, loading parameter, VSC-OPF

1. Introduction

In the transmission network for further commercial activity over and above already committed uses need for adequate computations of the available transfer capability in power systems, as this quantity has a direct effect on production and transmission cost signals. Realistic computations of ATC require considering various system limitations such as maximum loadability, bus voltage and transmission current limits as well as reactive and active power generator limits, as indicated in [1, 2, 3]. The current paper presents the computation of the ATC for the Italian system for a given loading and generation pattern which is of particular interest, using similar computational strategies as those used in [1, 4, 5], i.e., techniques based on determining voltage stability limits directly associated to voltage collapse conditions (saddle-node bifurcations), while considering most realistic system limits. It is a well known fact that transmission system power capabilities, and hence the system ATC, can be directly influenced by shunt and series compensation [6]. In [7], the author demonstrates the existence of optimal compensation levels and proposes the techniques to compute these values based on bifurcation theory. The appearance of Flexible AC Transmission System (FACTS) controllers, which are power-electronics-based devices designed for the direct control of ac transmission lines, is completely changing the way transmission systems are con- trolled and operated [8, 9]. Most FACTS controllers are basically based on variable shunt and/or series compensation of transmission systems; hence, it is important to study the effect of these controllers on ATC, so that design techniques can be developed to maximize ATC at minimum costs. This paper demonstrates the existence of optimal compensation levels of FACTS controllers and the

Received**:** November 2nd, 2013. Accepted: June 9th, 2014

techniques to compute these values based on bifurcation theory, continuation power flow (CPF) and sensitivity analysis. The concepts demonstrated in this paper are used here to indicate compensation levels that maximize the ATC of the IEEE 57-bus and 118-bus system. The optimal location of these controllers is determined in this paper using sensitivity of system loading factor and N-1 contingency criteria technique, as described in [11]. The techniques proposed in [11] are then used to design \optimal size" shunt and series FACTS controllers, specifically, the UPFC and GUPFC, that maximize ATC.
Section II describes the basic structure and operation of UPFCs and GUPFCs. This section also briefly presents all the basic concepts on which the analysis techniques presented here are based; In Section III, the techniques used for the optimal" design of the controllers are presented. Finally, Section IV presents the results of applying the proposed design techniques to the IEEE 57-bus and 118-bus system.

2. Basic Concept

The design techniques proposed in this paper are based on basic voltage stability concepts. A brief discussion of these concepts follows, together with a basic description of the operation, control and modeling of the two FACTS controllers, namely, the UPFC and the GUPFC, used throughout the paper.

A. Power Injection Model of the UPFC

A series inserted voltage and phase angel of inserted voltage can model the effect of UPFC on network. The inserted voltage has a maximum magnitude of $V_t = 0.1V_m$ where the V_m is rated voltage of the transmission line, where the UPFC is connected. It is connected to the system through two coupling transformers integrated into the model of the transmission line.
The whole UPFC model for representing power flow is depicted in Fig 1 [12].

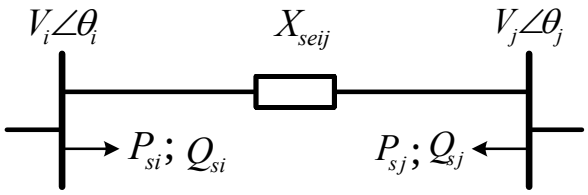

Figure 1. Complete injection model of UPFC

Where:
$P_{si} = rb_sV_iV_j\sin(\theta_{ij} + \gamma_{se})$; $Q_{si} = rb_sV_i^2\cos(\gamma_{se}) + Q_{inj\,sh}$; $P_{sj} = -rb_sV_iV_j\sin(\theta_{ij} + \gamma_{se})$; $Q_{sj} = -rb_sV_iV_j\cos(\theta_{ij} + \gamma_{se})$
$Q_{inj\,sh} = -i_qV_i$; V_i and V_j: bus voltages, X_{se}: equivalent series reactance, $b_s = 1/X_{se}$, P_{si}: real power injection on bus-i, P_{sj}: real power injection on bus-j, Q_{si}: reactive power injection on bus-i, Q_{sj}: reactive power injection on bus-j, $Q_{inj\,sh}$: reactive power injection by converter shunt

B. Power Injection Model of the GUPFC

A GUPFC model in power system is also the same as that the UPFC in steady-state. Furthermore, the GUPFC injection model can easily be incorporated in the steady-state power flow model. Since the series voltage source converter does the main function of the GUPFC, hence it is used as a material of discussion in the model. Suppose a series connected voltage source is located between nodes i and j and also i and k in a power system. The series voltage source converter can be modelled with an ideal series voltage $\bar{V}_{se\,in}$ in series with a reactance $X_{se\,in}$ (in Fig. 2) [13]

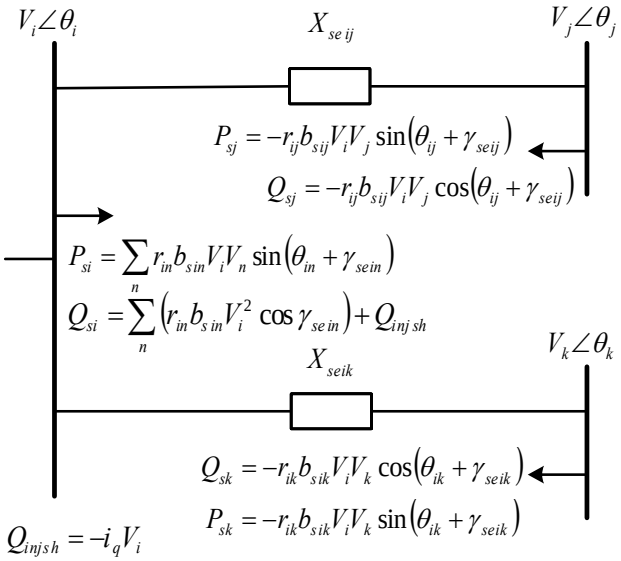

Figure 2. A complete injection model of the GUPFC

The reactive power delivered or absorbed by converter shunt is independently controllable by GUPFC and can be modelled as a separate controllable shunt reactive source. In view of above, $Q_{conv\,sh} = 0$. Consequently, the GUPFC injection model is constructed from the series connected voltage source model with the addition of a power equivalent to $P_{conv\,sh} + j0$ to node i. The shunt branch is used to supply active power injected to the system. Therefore, the amount of this active power must be added to the equation. The reactive power of the shunt converter can independently be controlled and modelled as a controllable shunt reactive power source. Since, for the sake the whole of injection reactive power to bus i $Q_{inj\,sh}$ suggested that it to be added to the series brunch model. Whole models are shown in Fig. 4. An injection active power to bus i P_{si} can be obtained by

$$P_{si} = \sum_n P_{conv\,se\,in} + \mathrm{Re}[S_{is}]$$
$$P_{si} = \sum_n r_{in}b_{s\,in}V_iV_n\sin(\theta_{in}+\gamma_{se\,in}) \quad (1)$$

A whole injection reactive power to bus i

$$Q_{si} = \mathbf{Im}[S_{is}] + Q_{inj\,sh}$$
$$Q_{si} = \sum_n (r_{in}b_{s\,in}V_i^2\cos\gamma_{se\,in}) + Q_{inj\,sh}$$
$$Q_{sh} = -i_qV_i \quad (2)$$

Active and reactive injection power to bus-n ($n = j, k, \ldots$) are

$$P_{sn} = -r_{in}b_{s\,in}V_iV_n\sin(\theta_{in}+\gamma_{se\,in}) \quad (3)$$
$$Q_{sn} = -r_{in}b_{s\,in}V_iV_n\cos(\theta_{in}+\gamma_{se\,in}) \quad (4)$$

C. Location of FACTS

The GUPFC use three or more converters and thus very expensive compared to the other FACTS controllers. The costs of some FACTS devices, the GUPFC and UPFC, are quite high especially those devices which use self-commuted converters. Therefore, it is very important to locate few devices optimally in the system for specific objectives or/and good performance.

This paper using the sensitivity of system loading factor and N-1 contingency criteria technique for finding an optimal location of the FACTS where to determine the system loading factor λ considering continuation power flow (CPF) and N-1 contingency criteria [11].

D. Voltage Collapse

Voltage stability in power systems has become a wide field of research. Voltage instability phenomena range time frames from seconds to hours and have been studied using a variety of static and dynamic models, including regulators and power electronics devices.

Topics relevant to the electricity market and optimal power flow techniques are the voltage collapse phenomena resulting from load changes and switching operations. Voltage collapse generally is a consequence of load increase in systems characterized by heavy loading conditions and/or when a change occurs in the system, such as a line outage. The results is typically that the current operating point, which is stable, \disappears" and the following system transient leads to a fast, unrecoverable, voltage decrease.

The most accepted analytical tool used to investigate voltage collapse phenomena is the bifurcation theory, which is a general mathematical theory able to classify instabilities, studies the system behavior in the neighborhood of collapse or unstable points and gives quantitative information on remedial actions to avoid critical conditions [15]. Voltage collapse studies and their related tools are typically based on the following general mathematical description of the system or in the bifurcation theory, it is assumed that system equations depend on a set of parameters together with state variables, as follows:

$$\begin{aligned} \dot{x} &= f(x, y, \lambda, p) \\ 0 &= g(x, y, \lambda, p) \end{aligned} \tag{5}$$

where $x \in \mathbb{R}^n$ represents the system state variables, corresponding to dynamical states of generators, loads, and any other time varying element in the system, such as FACTS controllers; $y \in \mathbb{R}^n$ corresponds to the algebraic variables, usually associated to the transmission system and steady-state element models, such as some generating sources and loads in the network. The parameters $\lambda \in \mathbb{R}^i$ stand for a set of non-controllable" parameters that drive the system to collapse, and typically represent the somewhat random changes in system demand. On the other hand, the parameters $p \in \mathbb{R}^k$ are used here to represent system parameters that are directly controllable, such as shunt and series compensation levels.

Then stability/instability properties are assessed varying \slowly" the parameters. In this paper, the parameter used to investigate system proximity to voltage collapse is the so called loading parameter $\lambda(\lambda \in \mathbb{R})$, which modifies generator and load powers as follows:

$$\begin{aligned} P_{G_1} &= (1 + \lambda)\left(P_{G_0} + P_S\right) \\ P_{L_1} &= (1 + \lambda)\left(P_{L_0} + P_D\right) \end{aligned} \tag{6}$$

Powers which multiply λ are called power directions. Equations (6) differ from the model typically used in continuation power flow analysis, i.e.

$$\begin{aligned} P_{G_2} &= P_{G_0} + \lambda P_S \\ P_{L_2} &= P_{L_0} + \lambda P_D \end{aligned} \tag{7}$$

where the loading parameter affects only variable powers P_S and P_D. In typical bifurcations diagrams voltages are plotted as functions of λ, i.e. the measure of the system loadability, thus obtaining the so called P-V or nose curves.

Based on (5), the collapse point may be defined, under certain assumptions, as the equilibrium point where the related system Jacobian is singular, i.e., the point $(x_0, y_0, \lambda_0, p_0)$ where

$$\begin{bmatrix} f(x_0, y_0, \lambda_0, p_0) \\ g(x_0, y_0, \lambda_0, p_0) \end{bmatrix} = F(z_0, \lambda_0, p_0) = 0 \tag{8}$$

and its Jacobian $D_z F|_0$ has a zero eigenvalue (or zero singular value). This equilibrium is typically associated to a saddle node bifurcation point. In addition, this voltage collapse index is specifically defined as the minimum singular value of the Jacobian.

E. Available Transfer Capability

In this paper, the ATC is more precisely defined as the maximum power that the system can transmit between areas of interest before the system collapses, while transmission system currents are kept within \realistic" limits, i.e., below thermal limits, at \reasonable" load voltage levels, as suggested by other authors, e.g., [2]. From the operational point of view, however, this is not the most appropriate definition, as in practice the system should not be allowed to get to the collapse point, or too close to it for that matter, due to the reduction in system stability margins. In this case an index such as the one defined in [1] would be more appropriate so that operators can monitor this value and take early action when it falls below certain thresholds. However, for this paper, the ATC definition proposed here is sufficient, since this value will be used only to evaluate the effect of different FACTS devices on the system ability to deliver a given power.

Definition of the ATC [16] is a measure of the transfer capability remaining in the physical transmission network for further commercial activity over and above already committed uses. Mathematically, ATC is defined as the Total Transfer Capability (TTC) less the Transmission Reliability Margin (TRM), less the sum of existing transmission commitments (which includes retail customer service) and the Capacity Benefit Margin (CBM). Total Transfer Capability (TTC) is defined as the amount of electric power that can be transferred over the interconnected transmission network in a reliable manner while meeting all of a specific set of defined pre- and post-contingency system conditions. Transmission Reliability Margin (TRM) is defined as that amount of transmission transfer capability necessary to ensure that the interconnected transmission network is secure under a reasonable range of uncertainties in system conditions. Capacity Benefit Margin (CBM) is defined as that amount of transmission transfer capability reserved by load serving entities to ensure access to generation from interconnected systems to meet generation reliability requirements.

ATC between areas can be calculated by increasing generation in the sending area and at the same time increasing the same amount of load in the receiving area until the power system reaches system limits in a while losses is minimized by the FACTS devices. The evaluation of ATC can be formulated as an optimization problem. The objective function to be maximized is basically expressed as

$$max \sum_{i \in area\ A} \Delta P_i \tag{5}$$
$$\dot{x} = f(x, y) \tag{6}$$
$$0 = g(x, y) \tag{7}$$
$$0 \le P_i + \Delta P_i \le P_{i_{max}} \tag{8}$$
$$-F_{max} \le F(x, y) \le F_{max} \tag{9}$$
$$V_{min} \le V \le V_{max} \tag{10}$$
$$EM(x, y) > 0 \tag{11}$$
$$0 \le V_{Ui} \le V_{Ui}^{max} \;;\; -\pi \le \alpha_{Ui} \le \pi \quad \text{for UPFC}$$
$$0 \le V_{GUin} \le V_{GUin}^{max} \;;\; -\pi \le \alpha_{GUin} \le \pi \quad \text{for GUPFC} \tag{12}$$

where P_i is power injection at the bus of generator $'i'$ and $\sum_{i \in area\ A} \Delta P_i$ is the sum of the increased generation in the sending area A, x is a vector of state variables and y is a vector of algebraic variables. Equation (6) represents differential equations describing the dynamic behaviours of the power system while (7) represents algebraic equations including power flow equations of the system and FACTS devices, operating and control constraint of the FACTS devices;. Equations (8)–(11) are inequality constraints. $P_{i_{max}}$ is the upper limit of active power output of generator $'i'$. F_{max} is the vector of thermal limits of transmission lines. V_{min} and V_{max}

are the vectors of lower and upper limits of bus voltage magnitudes, respectively. $EM(x, y)$ is energy margin which provides a quantitative measure of the degree of stability of power systems [14]. The energy margin of a power system indicates how far the power system is from the stability boundary. Equations (12) are limit for the UPFC and the GUPFC.
The limiting conditions of transmission systems can shift among thermal, voltage, and stability limits as the operating condition of the power system change over time. Stability limits of systems may become more restrictive than static limits depending on system operating conditions. The ATC calculation must be evaluated based on the most restrictive one of those limiting factors. Therefore, the accuracy of ATC calculation is not reliable if the stability limits of the system are not taken into account. It is desirable to consider stability limits in addition to static limits in the ATC calculation.

3. Analysis Techniques

As discussed, the definition of ATC used in this paper, for the purpose of designing FACTS controllers to \maximize" system transfer capability, is based on basic volt- age collapse concepts that are in turn grounded on bifurcation theory. The ATC is then formally defined here as the difference on active power owing into a system area between the base case and the voltage collapse (saddle-node bifurcation) point for a given generation and load pattern. Thus, to compute the ATC value, one has to first define the power transaction to be studied, i.e., the generation and load pattern, and then determine the voltage collapse point using any of the techniques developed to calculate this point; in this paper, the continuation power flow method is used to determine this point, as described in detailed in [4]. If there is no bifurcation point for the system under analysis, as in the case of the IEEE System with voltage dependent load model, the ATC will be defined as the maximum change in area power flow. A detailed description of the techniques used to determine the optimal location and size of the FACTS controllers to maximize the ATC can be used as defined in [11].

The techniques used here to determine the optimal location and size of the UPFCs and the GUPFC to increase ATC are based on the methodologies proposed in [4, 5, 10, 11].

A. Bifurcation Based Tools

In [7] studies in detail the effect of the controllable parameters *p* on the bifurcation behavior of equations (5), proposing a series of numerical techniques to compute the optimal values of p that maximize the \distance" to a bifurcation point. The paper demonstrates the advantages of maximizing this distance from the point of view of system stability, since the system becomes generally \more stable" as the distance to a bifurcation point is increased. In [10], used these basic concepts and some of the related numerical techniques to design FACTS controllers to maximize the system distance to collapse, and hence improve system stability.

In mathematical terms or in the critical solution terms, based on equation (8), Saddle-Node Bifurcation (SNB) conditions can be written as equation (13) or equation (14).

$$\begin{aligned} &f(z_c, \lambda_c, p_c) = 0 \\ &D_z f(z, \lambda, p)|_c \hat{v} = 0 \\ &\|\hat{v}\| = 1 \end{aligned} \tag{13}$$

$$\begin{aligned} &f(z_c, \lambda_c, p_c) = 0 \\ &\hat{w}^T D_z f(z, \lambda, p)|_c \hat{v} = 0 \\ &\|\hat{w}\| = 1 \end{aligned} \tag{14}$$

where the subscript c stands for the \critical solution at the bifurcation point, $\hat{v}$ and $\hat{w}$ are the right and the left eigenvectors respectively, and the Euclidean norm is used for the $\|\cdot\|$ operator. The Euclidean norm reduce the sparsity of the Jacobian matrix, but allows avoiding refactorizations (which is needed in the case of $\infty - \text{norm}$) and appears to be numerically more

stable than the $1-$ norm. In this paper\static" SNBs will be considered, i.e. state variables are only the power flow variables *x* in (6).
Together with SNBs, also Limit-Induced Bifurcations (LIB) can cause voltage collapse. LIBs are caused by a change in system equations, typically when maximum generator reactive power limits are reached. At a LIB, one generator switches from a PV bus with controlled voltage $V_G = V_{G_0}$ to a PQ bus, where $Q_G = Q_{G_{max}}$. Observe that LIBs might be or not be a catastrophic event, since are not necessarily associated with a maximum loading condition. The LIB can be viewed as the solution of the system:

$$0 = f(z_c, \lambda_c, p_c)$$
$$0 = f^*(z_c, \lambda_c, p_c) \quad (15)$$

where f and f^*, are the initial and the changed system equations and control variables, respectively.

SNBs and LIBs may occur for unacceptable values of some bus voltages, i.e. for voltages below security bounds (typically 0.95 or 0.9 p.u.), or other limits which may lead to unfeasible operating point (e.g. thermal limits on transmission lines). In order to provide realistic results, voltage stability analysis has to take into account all physical constraints. Furthermore, that several thermal and voltage limits occur well before reaching the LIB associated with the maximum loading parameter λ_{max}, thus significantly reducing the feasible loadability of the network λ_c.

B. Available Loading Capability

SNBs and LIBs (and possibly thermal or voltage security limits) may be associated to the system maximum loadability or Maximum Loading Condition (MLC) [4], which can be defined as follows:

$$\text{MLC} = (1+\lambda_c)\sum_{j\in\mathcal{J}} P_{L_1} = (1+\lambda_c)\left(\sum_{j\in\mathcal{J}} P_{L0_j} + \sum_{j\in\mathcal{J}} P_{D_j}\right) \quad (16)$$

where λ_c is the \critical" value of the loading parameter at the bifurcation point or security limit. Let us define the concept of Available Loading Capability (ALC) as follows:

$$\text{ALC} = \text{MLC} - \sum_{j\in J} P_{L_j} = \text{MLC} - \text{TTL} \quad (17)$$

where TTL is the Total Transaction Level at the current operating point. Thus, in terms of λ_c, one has:

$$\text{ALC} = \lambda_c \sum_{j\in J} P_{L_j} = \lambda_c \text{TTL} \quad (18)$$

ALC values will be used in this paper as a measure of the security margin of the current operating point with regard to voltage stability criteria.

The definition of ALC given in (18) is actually incomplete, since first class emergency contingencies, i.e. an N-1 contingency criterion, are not taken into account. As it might be expected, line outages may drastically reduce the values of λ_c and MLC. In North American power companies, system operators follow the definition of Available Transfer Capability as proposed by NERC. The ATC is computed with the following expression:

$$\text{ATC} = \text{TTC} - \text{ETC} - \text{TRM} \quad (19)$$

Where $\text{TTC} = min\left(P_{max_{I_{lim}}}, P_{max_{V_{lim}}}, P_{max_{S_{lim}}}\right)$ represents the Total Transfer Capability, i.e. the maximum power that the system can deliver given the security constraints defined by

thermal limits (I_{lim}), voltage limits (V_{lim}) and stability limits (S_{lim}) based on an N-1 contingency criterion, ETC stands for the Existing Transmission Commitments, and TRM is the Transmission Reliability Margin, which is meant to account for uncertainties in system operations. TRM is usually assumed to be a fixed quantity, i.e. TRM = K, where K is a given MW value used to represent contingencies that are not being considered during the ATC computations (e.g. N-2 contingencies). In this paper, TRM is ignored without loss of generality, since it would affect the MLCs resulting from the proposed OPF solutions only for an offset value.

The ATC is a basic concept typically associated with \area" interchange limits which are imposed by transmission rights, and is used as a measure of available power which can be further exchanged among different entities. In System wide" ATC (SATC), and corresponding \System wide" TTC, ETC and TRM are proposed to extend the ATC concept to a system domain.

In this paper, stayed away from the debate whether the ATC has to be defined only for area exchange limits or can be extended to system wide information on the security margin. However, the structure of the NERC definition of ATC to define an available loading condition which includes N-1 contingency is used, namely $\text{ALC}^{(N-1)}$. Based on (17) and (19), the following correlations can be stated as

$$\text{ETC} \Rightarrow \text{TTL} \tag{20}$$

and

$$\text{TTC} \Rightarrow \text{MLC}^{(N-1)} = \left(1 + \min_h\{\lambda_{c_h}\}\right)\text{TTL} \tag{21}$$

where $\text{MLC}^{(N-1)}$ is the MLC associated with the line outage h which leads to the minimum λ_c. $\text{MLC}^{(N-1)}$ is the SNB point of the nose curve associated with contingency on a line. Thus, from (19), the definition of ALC is as follows:

$$\text{ATC} \Rightarrow \text{ALC}^{(N-1)} = \min_h\{\lambda_{ch}\}\sum_{j\in J} P_{L_j} = \min_h\{\lambda_{ch}\}\,\text{TTL} \tag{22}$$

Furthermore, according to [20] in term loadability and increasing power transfer that the generation can be seen as follows

$$\sum_{i=1}^{n_g} P_{g_i} = \sum_{i=1}^{n_g}\left(P_{G0_i} + \lambda P_{S_i}\right) \tag{23}$$

and the supply should equal total demand plus losses, i.e.

$$\sum_{i=1}^{n_g} P_{S_i} = P_D + P_{\text{Losses}} \quad ; P_{\text{Losses}} = P_{L0} \tag{24}$$

and can be written as.

$$\sum_{i=1}^{n_g} P_{S_i} = \sum P_{L_i} \tag{25}$$

Since, the P_{L0} can be minimized by the FACTS devices that installed at the best location in an optimal location), therefore will be maximizing the λ_c that will influence and increase power transfer or the power flow, because the level of loadability or the level of critical condition (λ_c represents the maximum loadability of the network where this value viewed as the measure of the congestion of the network [21]) will be decreased. While, in the same manner for the demand P_D can be arranged as

$$P_D = P_L - P_{L_o} \tag{26}$$

where P_D will increase if $P_{L_o}$is minimized by the FACTS therefore can enhance the ATC as well as power flow.

C. Sensitivity Analysis

As presented in [4], that continuation power flow analysis may also be used to get a variety of \sensitivity" factors of the current or critical points with respect to the loading parameter. It has been said that, at a SNB point, the sensitivity with respect to λ of a variable is infinite. This actually does not necessarily imply a huge variation of the variable itself. However, sensitivity factors can be used to determine which variable (typically a \control" variable), at the operating point is mostly affected by the parameter variation, and thus varying that variable is likely a good \direction" toward stability improvement. Since the sensitivity analysis is basically a linearization around a current steady state point and power system models are highly nonlinear, variation steps of control variables cannot be huge. It is thus necessary to repeat the computation of sensitivity factors after each step (an example of iterative techniques to optimize transmission congestion in simple auction-based markets with respect to voltage stability criteria has been proposed).

First, a basic VSC-OPF solution that does not consider contingencies is used for determining the sensitivity of power flows with respect to the loading parameter λ_c. Then, based on this solution and assuming a small variation ε of the loading parameter and re-computing the power flows by solving f_c, normalized sensitivity factors can be approximately computed as follows:

$$\boldsymbol{p_{hk}} = \boldsymbol{P_{hk}} \frac{\partial \boldsymbol{P_{hk}}}{\partial \lambda_{\boldsymbol{c}}} \approx \boldsymbol{P_{hk}}(\lambda_{\boldsymbol{c}}) \frac{\boldsymbol{P_{hk}}(\lambda_{\boldsymbol{c}}) - \boldsymbol{P_{hk}}(\lambda_{\boldsymbol{c}} - \varepsilon)}{\varepsilon} \tag{27}$$

Where $\boldsymbol{p_{hk}}$ and $\boldsymbol{P_{hk}}$ are are the sensitivity factor and the power flows of line *h-k* respectively. The scaling is introduced for properly evaluating the \weight of each line in the system, and thus for considering only those lines characterized by both significant" power transfers and the high sensitivities where significantly is influenced by injection model or injection mechanism of the FACTS devices.

The first lines with the biggest sensitivity factors $\boldsymbol{p_{hk}}$ are selected (from multiple tests, 5 lines appear to be a sufficient number), and a VSC-OPF for each one of these contingencies is solved (may be done in parallel). The VSC-OPF solution that presents the lowest $\mathrm{ALC}^{(N-1)}$ is chosen as the final solution. Observe that not necessarily the outage of the line with the highest sensitivity factor will always produce the lowest $\mathrm{ALC}^{(N-1)}$, because of the non-linear nature of the voltage stability constraints in multi-objective VSC-OPF; hence the need of solving more than one VSC-OPF problem. However, ranking the sensitivity factors leads generally to determine a reduced number of critical areas; $\mathrm{ALC}^{(N-1)}$s associated with outages of high sensitivity lines within a certain area generally show only small differences. Thus, in practice, one needs to evaluate only one contingency constrained VSC-OPF for each critical area that was determined by the sensitivity analysis.

Observe that line outages that cause a separation in islands of the original grid have to be treated in a special way, since the multi-objective VSC-OPF may not converge. In order to solve this problem, the islanded market participants are not committed and the fixed power productions and/or absorptions eliminated. This solution appears to be reasonable especially for realistic transmission grids, which are typically well interconnected, as generally only very few buses result islanded as the consequence of a line outage.

In other way, a diagonal matrix whose an elements are the singular values of Jacobian matrix J, ordered in ascending order, it is possible to determine the influence of any control parameter *p* on the minimum singular value of J (or on the maximum singular value). Thus, following a change about a given equilibrium point. To evaluate the sensitivities of the

minimum singular value with respect to power injections in the load flow equations, J becomes the unit matrix. On the other hand, if p corresponds to a branch admittance used to evaluate the effect of series compensation in the load flow equations, J presents four nonzero elements corresponding to the P and Q mismatch equations at the two buses i and j connected by the branch.

As a final remark, it should be noted that the sensitivity or contingency analysis technique discussed here can also be associated with a continuation power flow analysis, thus avoiding the need of running a CPF routine for each line outage as it was stated in the previous section. It also has been successfully used to rank contingencies, and is adopted here to evaluate, from the voltage collapse point of view, optimal locations of shunt and series compensation. It is important to mention that the procedure proposed here to determine the most suitable bus/branch for the insertion of the UPFC or the GUPFC needs neither the definition of the collapse point nor the definition of the system load change pattern; hence, this technique can be directly applied to the case where the system does not present a bifurcation. This is one of the main advantages of this technique, and has been confirmed in several studies by basically obtaining the same results when the sensitivities or the contingencies are computed at the initial loading conditions as when these are computed at the collapse point.

4. Results

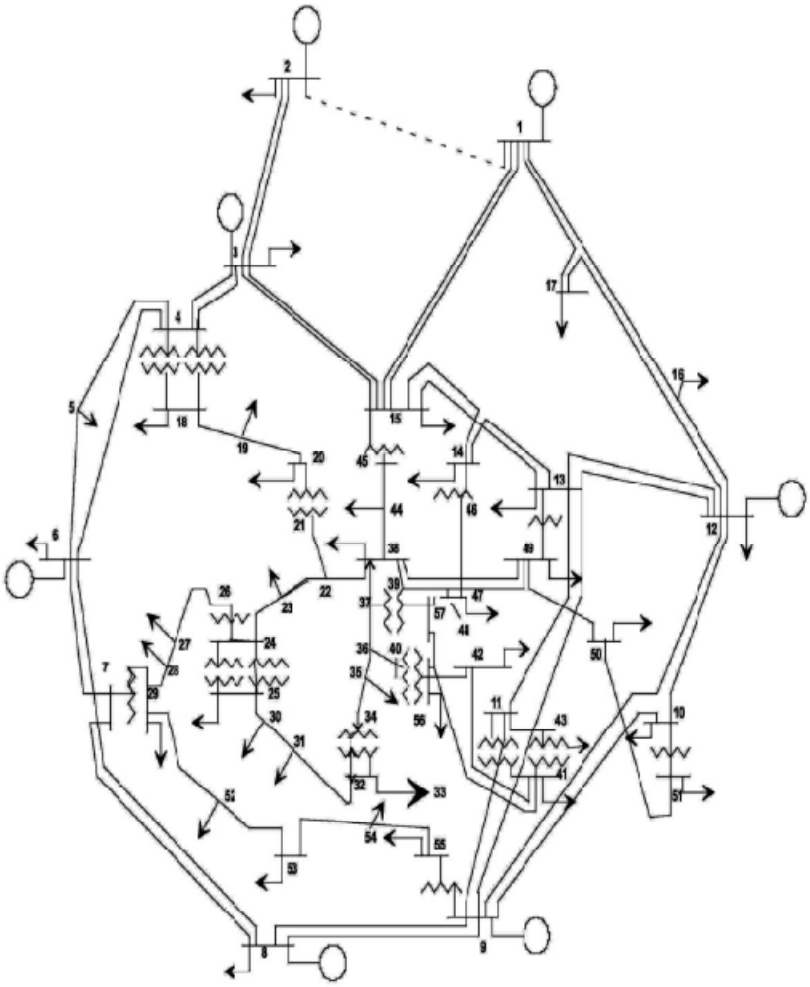

Figure 3. IEEE 57-bus test system

All the results discussed here were obtained in Matlab [17] using the nonlinear predictor-corrector primal-dual interior-point method based on the Mehrotra's predictor-corrector technique [18] where coded in the Power System Analysis Toolbox (PSAT) [19] and modified by the means of implementation of the VSC-OPF with N-1 contingency criteria installed the FACTS devices techniques. Furthermore, Figure 3 depicts the IEEE 57-bus test case, redrawn from [22] by [23], and Figure 4 depicts the IEEE 118-bus test case, redrawn from [22] by [24], then the data modified in this paper representing generation companies (GENCOs) and energy supply companies (ESCOs) that provide supply and demand bids, respectively.

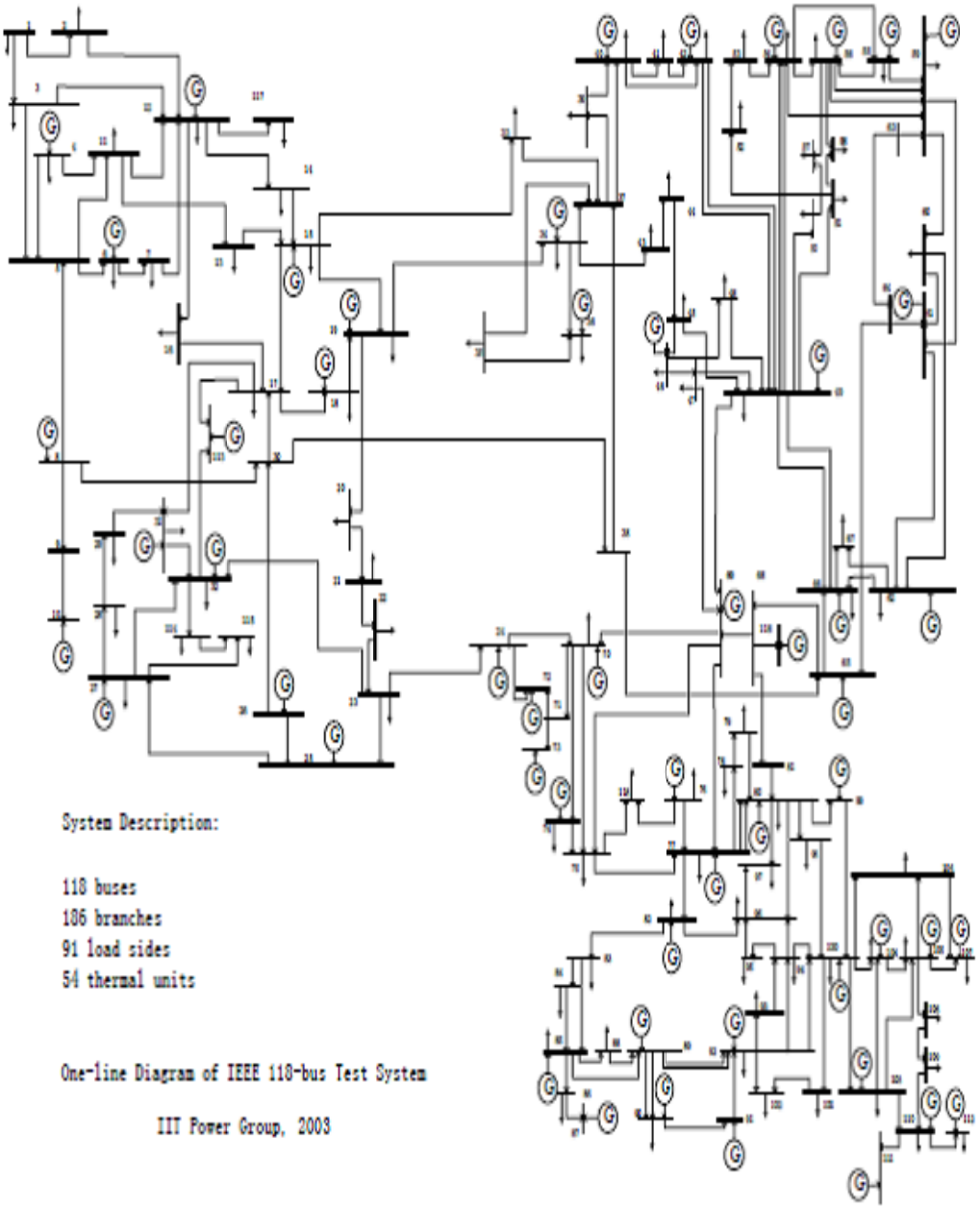

Figure 4. IEEE 118-bus test system

All Q and S limits on generators as well as limits on the UPFC and GUPFC controllers were enforced for the ATC computations in all cases. On the other hand, bus voltage and current limits were only monitored and not strictly enforced, as some of these limits overly constrained the transmission system voltages and currents, yielding rather conservative results. The allocation of the FACTS using theory which is related to the sensitivity and contingency analysis, since the ATC definition used in this paper is related to the maximum power exchange between areas before voltage collapse occurs, it is reasonable to assess the quality of a candidate bus/branch by means of voltage collapse related indices or sensitivities.

Table 1. Sensitivity of system loading factor and N-1 contingency criteria results for IEEE 57-bus.

Line	*Bus*	*Pij [p.u.]*	*c1 [p.u.]*	*c2 [p.u.]*	*C3 [p.u.]*	*C4 [p.u.]*
6	6-7	0.5677	0.5794	-6.0955	0.08416	-0.8854
7	6-8	0.9313	0.9505	-9.9998	0.05025	-0.5287
8	8-9	3.2623	3.3295	-35.028	0.27683	-2.9124
9	9-10	0.3893	0.3973	-4.1799	0.1201	-1.2635
10	9-11	0.5381	0.5492	-5.7778	0.0675	-0.7101
11	9-12	0.1854	0.1892	-1.9904	0.14404	-1.5153
12	9-13	0.4012	0.4095	-4.3081	0.10023	-1.0545
22	7-8	1.4269	1.4563	-15.321	0.14331	-1.508
41	7-29	0.8356	0.8528	-8.9721	0.12229	-1.2875
80	9-55	0.2136	0.2180	-2.2937	0.13426	-1.4125

Table 2. Sensitivity of system loading factor and N-1 contingency criteria results for IEEE 118-bus.

Line	*Bus*	*Pij [p.u.]*	*c1 [p.u.]*	*c2 [p.u.]*	*C3 [p.u.]*	*C4 [p.u.]*
7	8-9	5.3397	5.3409	-19.05	0.23407	-0.8349
8	8-5	4.064	4.065	-14.50	1.4463	-5.1591
9	9-10	5.3966	5.3978	-19.26	-0.4777	1.7044
21	15-17	1.2614	1.2616	-4.501	0.25828	-0.9213
22	16-17	0.2110	0.21106	-0.753	-0.0019	0.00684
23	17-18	0.9583	0.95852	-3.419	0.28141	-1.0039
36	30-17	2.7682	2.7688	-9.877	1.0898	-3.8874
51	38-37	2.9311	2.9317	-10.46	1.265	-4.5125
96	38-65	2.2242	2.2247	-7.936	-0.0545	0.19425
97	64-65	2.2062	2.2067	-7.872	0.49347	-1.7603
141	89-92	2.433	2.4336	-8.681	0.36455	-1.3005
183	68.12	2.2423	2.2428	-8.001	0.63648	-2.2705

The following are alternatively to the methods described above for determining most suitable buses for the installation of the shunt part and the most appropriate branches for placing the series part, one may use the sensitivity and contingency analysis as proposed here. In the system 57-bus the sensitivity of system loading factor value is in Line-8 in Table 1 where it is the best FACTS with allocate the UPFC in Line-8 and Pod at Line-7 compared with the GUPFC in Line-9, Line-10, Line-11, Line-12, Line-80 and Pod at Line-8.

In the system 118-bus the sensitivity of system loading factor value is in Line-7 and Line-9 in Table 2 where it is the best FACTS with allocate the UPFC in Line-9 and Pod at Line-7 compared with the GUPFC in Line-7 and Line-9 with Pod at Line-8.

Table 3 Solution statistic for 57-bus and 118-bus without FACTS.

Solution Statistic	*57-Bus Without FACTS*		*118-Bus Without FACTS*	
	PF	*OPF*	*PF*	*OPF*
Obj. Fun.	-	6357.1244	-	-5478.3333
Active Limits:	-	59	-	1724
Iteration	4	20	4	21
Barrier Parameter	0	0	0	0.00288
Vari. Mismatch	0	8e-05	0	5.6498
PFE Mismatch	0	0	15,1291	2.1396
Weighting Factor	-	0.1	-	0.1
Load [MW]	1250,8	-	3668	-
Load [Mvar]	336,4	-	1438	-
Gen [MW]	1275,131	-	3800.9725	-
Gen. [MVar]	289,0738	-	880.0858	-
Losses [MW]	24,331	17.592	132.9725	175.695
Losses [MVar]	-25,7134	-	-557.9142	-
Demand [MW]	-	58	-	1880.3487
IMO Pay [$/h]	-	409.7391	-	4799.9144
Lambda	-	0.1	-	0.07647
MLC [MW]	-	1439.68	-	5972.615
ALC[MW]	-	130.88	-	424.2663
TTL [MW]	-	1308.8	-	5548.3487
ATC [MW]	1439.68 (OPF-CPF) 1447.9591 (sensitivity analysis)		5915.1207 (OPF-CPF) 5924.4139 (sensitivity analysis)	

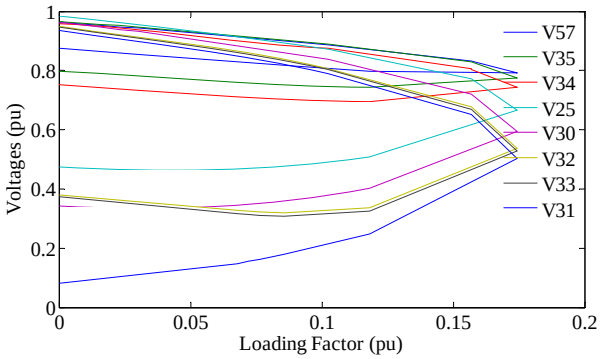

Figure 5. The nose curves (P-V curves) of IEEE 57-bus system without FACTS for different buses

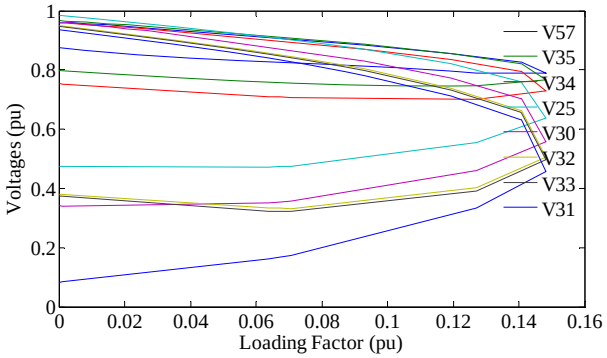

Figure 6. The nose curves (P-V curves) of IEEE 57-bus system with UPFC for different buses

Table 4. Solution statistic for 57-bus with UPFC and GUPFC.

Solution Statistic	*With UPFC*		*With GUPFC*	
	PF	*OPF*	*PF*	*OPF*
Obj. Fun.	-	34017739.8	-	264601.6066
Active Limits:	-	676	-	676
Iteration	4	21	4	21
Barrier Parameter	0	1	0	1
Vari. Mismatch	0	210970062	0	959413461.1
PFE Mismatch	613,9	0.79782	15,1291	0.80763
Weighting Factor	-	0.1	-	0.1
Gen [MW]	1267,226	-	1274,201	-
Gen. [MVar]	284,951	-	302,8665	-
Losses [MW]	16,4261	7.674	23,4006	11.736
Losses [MVar]	-29,8361	-	-11,9213	-
Demand [MW]	-	172.2242	-	199.4764
IMO Pay [$/h]	-	16637324.9	-	-86818.8656
Lambda	-	0.07341	-	0.07914
MLC [MW]	-	1527.4814	-	1565.0515
ALC[MW]	-	104.4572	-	114.775
TTL [MW]	-	1423.0242	-	1450.2764
ATC [MW]	1525.8371 (OPF-CPF) 1508.2731 (sensitivity analysis)		1567.3234 (OPF-CPF) 1532.3244 (sensitivity analysis)	

Table 5 Solution statistic for 118-bus with UPFC and GUPFC.

Solution Statistic	*With UPFC*		*With GUPFC*	
	PF	*OPF*	*PF*	*OPF*
Obj. Fun.	-	-9821.327	-	-8303.1449
Active Limits:	-	1724	-	1724
Iteration	4	21	3	21
Barrier Parameter	0	0.00184	0	0.00248
Vari. Mismatch	0	1.5474	0	2.2372
PFE Mismatch	613,9	1.3876	9.4244	1.7182
Weighting Factor	-	0.1	-	0.1
Gen [MW]	3796.0389	-	3800.8958	-
Gen. [MVar]	997.4784	-	882.5299	-
Losses [MW]	128.0389	127.189	132.8958	128.198
Losses [MVar]	-440.5216	-	-555.4701	-
Demand [MW]	-	1554.9936	-	1682.1353
IMO Pay [$/h]	-	4184.9452	-	4109.4857
Lambda	-	0.09065	-	0.08548
MLC [MW]	-	5696.4709	-	5807.4734
ALC[MW]	-	473.4773	-	457.3381
TTL [MW]	-	5222.9936	-	5350.1353
ATC [MW]	5696.4709 (OPF-CPF) 5697.0818 (sensitivity analysis)		5807.4734 (OPF-CPF) 5812.8806 (sensitivity analysis)	

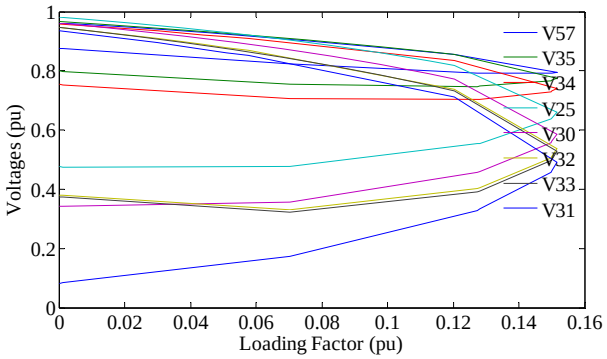

Figure 7. The nose curves (P-V curves) of IEEE 57-bus system with GUPFC for different buses

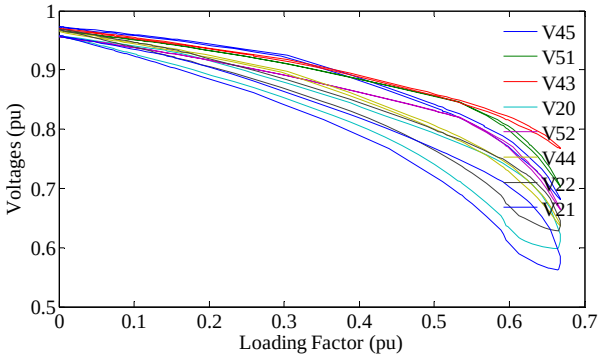

Figure 8. The nose curves (P-V curves) of IEEE 118-bus system without FACTS for different buses

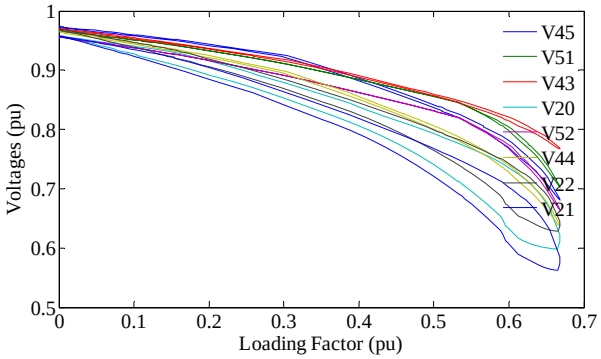

Figure 9. The nose curves (P-V curves) of IEEE 118-bus system with UPFC for different buses

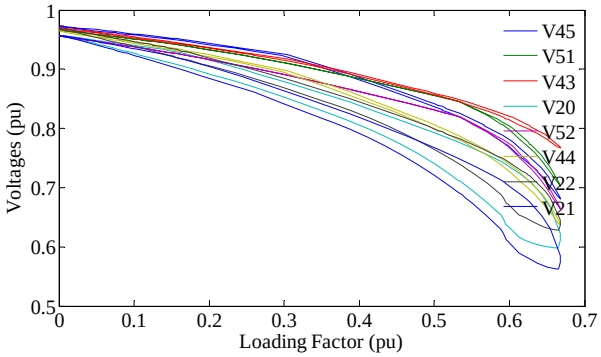

Figure 10. The nose curves (P-V curves) of IEEE 118-bus system with GUPFC for different buses

Figure 5 depicts the nose curve or the bifurcation diagram of IEEE 57-Bus without installed FACTS with V (voltages) versus λ (loading factor), show λ_{min}=0, λ_{max}=0.1743; V_{min}= 0.7913 V_{max}= 0.9621. The system presents a collapse point at the maximum value of λ (loading factor) which corresponds to a maximum total loading condition of 1439.68 MW and an ATC of 1439.68 (with OPF-CPF) or 1447.9591 (with sensitivity analysis) MW as can be seen in Table

3; for this kind of load model, the value of λ can be directly associated to the total MW loading. It is interesting to notice that the maximum power transfer from the one to the other area, which does not correspond to the ATC in this case, does not occur at the collapse or maximum loading point, but on the lower (\unstable") side of the bifurcation diagram. Observe that LIBs might be or not be a catastrophic event, since are not necessarily associated with a maximum loading condition.

Figure 6 depicts a nose curve of IEEE 57-Bus with installed the UPFC with V versus λ, show λ_{min}=0, λ_{max}=0.1484; V_{min}=0.7889, V_{max}= 0.9621. The system presents a collapse point at the maximum value of λ (loading factor) which corresponds to a maximum total loading condition of 1527.4814 MW and an ATC of 1525.8371 (with OPF-CPF) or 1508.2731 (with sensitivity analysis) MW as can be seen in Table IV; for the same as system without FACTS of load model, the value of λ can be directly associated to the total MW loading. As explained for the system without FACTS above, it also is interesting to notice that the maximum power transfer from the one to the other area, which does not correspond to the ATC in this case, does not occur at the collapse or maximum loading point, but on the lower (\unstable") side of the bifurcation diagram. Observe that LIBs might be or not be a catastrophic event, since are not necessarily associated with a maximum loading condition. In this case, the ATC or performances of the system are shown increase better than without FACTS.

Figure 7 depicts a nose curve of IEEE 57-Bus with installed the GUPFC with V versus λ, show λ_{min}=0, λ_{max}=0.1517; V_{min}=0.7923, V_{max}= 0.9619. The system presents a collapse point at the maximum value of λ (loading factor) which corresponds to a maximum total loading condition of 1565.0515 MW and an ATC of 1567.3234 (with OPF-CPF) or 1532.3244 (with sensitivity analysis) MW as can be seen in Table 4; for the same as system above of load model, the value of λ can be directly associated to the total MW loading. As explained about performance in Figure 2 for the system with the UPFC above, in this case, the ATC or performances of the system are shown increase better than with the UPFC.

Figure 8 depicts a nose curve of IEEE 118-Bus without installed FACTS with V versus λ, show λ_{min}=0, λ_{max}=0.6677; V_{min}= 0.6808, V_{max}= 0.9737. The system presents a collapse point at the maximum value of λ (loading factor) which corresponds to a maximum total loading condition of 5972.615 MW and an ATC of 5915.1207 (with OPF-CPF) or 5924.4139 (with sensitivity analysis) MW as can be seen in Table 3.

Figure 9 depicts a nose curve of IEEE 118-Bus with installed the UPFC with V versus λ, show λ_{min}=0 , λ_{max}=0.6677; V_{min}= 0.6808, V_{max}= 0.9737. The system presents a collapse point at the maximum value of λ (loading factor) which corresponds to a maximum total loading condition of 5696.4709 MW and an ATC of 5696.4709 (with OPF-CPF) or 5697.0818 (with sensitivity analysis) MW as can be seen in Table 5.

Figure 10 depicts a nose curve of IEEE 118-Bus with installed the GUPFC with V versus λ, show λ_{min}=0, λ_{max}=0.6677; V_{min}= 0.6808, V_{max}= 0.9737. The system presents a collapse point at the maximum value of λ (loading factor) which corresponds to a maximum total loading condition of 5807.4734 MW and an ATC of 5807.4734 (with OPF-CPF) or 5812.8806 (with sensitivity analysis) MW as can be seen in Table 5.

As shown the results above Figure 8, Figure 9 and Figure 10 gave the same as figures and data statistic that indicating the candidate buses have basically the same effect on the ATC as the one proposed here, however gave differ maximum total loading condition, ATC and the other results, as shown in Table 3, Table 4 and Table 5 where the GUPFC gave better Barrier Parameter, variable mismatch, PFE Mismatch, generation, lambda and MLC. Furthermore, gave lower losses and independent market operator (IMO) pay, therefore can be expressed that applying the GUPFC controller is better than the UPFC or without FACTS in 118-Bus system.
According to the equations of injection model of the UPFC and GUPFC as shown in Figure 1 and Figure 2 and the equation (7) that the UPFC and GUPFC can influence the system in controlling or enhancement the ATC as good as power flow possible. These phenomena are shown in Table 4 and Table 5 compared with Table 3 that are especially signed by enhancing TTL, ALC Lambda and MLC. According to the phenomena, the GUPFC can so strong

influence the system in controlling or enhancement the ATC is compared with the UPFC, because it have series injections in more than one line leaving the bus so that give balance injection voltage for lines, therefore give better controlling effect and result both lower losses and better power flow controlling for whole system then the UPFC. Finally, The GUPFC give better voltage stability “system security”, dynamic stability and ATC than the UPFC.

5. Conclusions

This paper discusses in proper techniques to locate UPFC and GUPFC controllers from the ATC point of view, and tests the proposed methodologies in a system. In this paper the GUPFC gave better controller than the UPFC or without FACTS controller. The GUPFC can so strong influence the system in controlling or enhancement the ATC as good as power flow possible is compared with the UPFC. These techniques can be also applied to other FACTS controllers used for shunt and series compensations.

The paper also demonstrates that both sensitivity and contingency analysis information obtained from collapse studies yield basically the same results, which can then be used to determine optimal control parameters to improve system operation. It is important to highlight the fact that the studies presented in this paper are based on steady state techniques, and may be consideration is given here to the dynamic response of the system, which in some cases could also be on the design process of FACTS controllers.

The system presented has a unique opportunity to develop and test new techniques for the integral design of FACTS controllers where one can readily determine the sensitivities of a voltage collapse index based on singular values with respect to various system parameters, which in this case are the reactive power injections, by the shunt branch, and the branch admittances, by series branch as which the property of the UPFC and GUPFC.

6. References

[1] R. P. Klump and T. J. Overbye,, “\A transmission-based voltage stability measure for available transfer capability (atc) calculations," *Proc. NAPS, MIT, pp. 351-357, November 1996.*

[2] C. A. Ayasum and R. Fischl,, “On the region-wise analysis of available transfer capability (atc)," *Proc. NAPS, Wyoming, pp. 464-469, October 1997.*

[3] G. Gross, “editor, Proc. Workshop on ATC, University of Illinois”, *Urbana-Champaign, IL, June 1997*.

[4] F. Milano, “Pricing System Security in Electricity Market Models with Inclusion of Voltage Stability Constraints”, *Ph.D. Thesis, Electrical Engineering, University of Genova, Genova, Italy, 2003*.

[5] F. Milano, C. A. Cañizares, M. Invernizzi, “Voltage Stability Constrained OPF Market Models Considering N-1 Contingency Criteria,” *Electric Power Systems Research, Vol. 74, No. 1, pp. 27-36, April 2005*.

[6] A. R. Bergen, “Power Systems Analysis”. *Prentice-Hall, New Jersey, 1986*.

[7] C. A. Canizares, ”Calculating optimal system parameters to maximize the distance to saddle-node bifurcations," *IEEE Trans. Circuits and Systems-I, vol. 45, no. 3, pp. 225-237, 1998*.

[8] N. G. Hingorani, ”Flexible ac transmission systems," *IEEE Spectrum, pp. 40-45, April 1993*.

[9] D. Maratukulam, editor, Proc. FACTS Conference I, “The Future in High-voltage Transmission”, *TR-100504, EPRI, March 1992*.

[10] C. A. Canizares and Z. T. Faur, ”Analysis of SVC and TCSC controllers in voltage collapse," *IEEE/PES PE-200-PWRS-0- 2-1998, accepted for publication in IEEE Trans. Power Systems, March 1998*.

[11] R.S. Lubis, S.P. Hadi and Tumiran, “Selection of Suitable Location of the FACTS Devices for Optimal Power Flow” *International Journal of Electrical & Computer Science IJECS-IJENS Vol. 12 No. 03, pp38-49, June, 2012*.

[12] M. Norozian, L. Angquist, M. Ghandhari and G. Andersson, “Use of UPFC for Optimal Power Flow Control”, *IEEE Trans. Power Delivery, vol. 12, no. 4, pp.1629-1634, 1997*.
[13] R. S. Lubis, S. P. Hadi and Tumiran, “Modeling of the Generalized Unified Power Flow Controller for Optimal Power Flow”, *Proceedings of the 2011 International Conference on Electrical Engineering and Informatics, July 17-19, 2011, Bandung Indonesia, Vol. 3, pp. 1616-1621, 2011*.
[14] Fouad, A. A. and Vittal, V., “Power System Transient Stability Analysis Using the Transient Energy Function Method”, *Englewood Cliffs, NJ: Prentice-Hall, 1992*.
[15] R. Seydel, “Practical Bifurcation and Stability Analysis: From Equilibrium to Chaos”, *Second Edition, Springer-Verlag, New York, 1994*.
[16] NERC, \”Available Transfer Capability Definition and Determination", *Tech.Rep., NERC, USA, 1996*.
[17] Natick, MA, 2012, “MATLAB Programming Fundamentals”, *the MathWorks, Inc., USA, [Online] Available at* http://www.mathworks.com.
[18] V.H. Quintana, G.L. Torres, “Introduction to interior-point methods,” *IEEE PICA, Santa Clara, CA, 1999*.
[19] F. Milano, "An Open Source Power System Analysis Toolbox", *IEEE Trans. on Power Systems, Vol. 20, No. 3, pp. 1199-1206, August 2005*.
[20] R. S. Lubis, S.P. Hadi and Tumiran “Optimal Power Flow Enhancement Considering Contingency with Allocate FACTS”, *International Journal of Energy Engineering, Scientific & Academic Publishing SAP USA, Vol. 3, No. 6, December 2013*.
[21] F. Milano, C.A. Ca˜nizares, M. Invernizzi, “Multi-objective optimizationfor pricing system security in electricity markets,” *IEEE Trans. Power Syst. 18 (2) (2003) 596–604*.
[22] R. Christie, "Power System Test Archive." *[Online] Available at* www.ee.washington.edu/research/pstca/.
[23] Simulation results and discussion, Chapter-5 pp. 188-232 *[Online] Available at* http://shodhganga.inflibnet.ac.in/bitstream/10603/4566/15/15_chapter%205.pdf.
[24] IIT Power Group, 2003, *[Online] Available at* http://www.geocities.jp/ps_dictionary/simulation/IEEE118bus_figure.pdf

Rakhmad Syafutra Lubis was born in Padang Sidempuan, North Sumatera, Indonesia, on January 05, 1969. He received B.Sc. degree from Department of Electrical Engineering, Universitas Sumatera Utara Medan, Indonesia in 1997 and M.Eng. degree from Department of Electrical Engineering, Universitas Gadjah Mada, Yogyakarta, Indonesia in 2003. He is currently pursuing the Ph.D. degree in the Electrical Engineering Department at the Universitas Gadjah Mada, Yogyakarta, Indonesia, in the field of power system control and optimizaton. He is a Lecturer in the Department of Electrical Engineering, Faculty of Engineering, Universitas Syiah Kuala, Banda Aceh, Indonesia. His research interests are in Power System Restructuring /Deregulation, FACTS Technology, Optimal Power Dispatch and Security Analysis, Power System Dynamics Operation and Control, Power System Planning and Demand Side Management, Application of Genetic Algorithms and Interior Point Algorithm in Power Systems.

Sasongko Pramono Hadi is lecturer in The Department of Electrical Engineering and Information Technology, Faculty of Engineering, Gadjah Mada University, Yogyakarta, Indonesia. He was born in Klaten, December 27, 1953. In 1979, he received Bachelor degree in Electrical Engineering, Gadjah Mada University, Yogyakarta, Indonesia. He obtained Master and Doctoral degree in 1985 and 1988 respectively, in Electrical Engineering, with research subject: Power System Adaptive Control, from The Institute Nationale Polytechnique de Grenoble (INPG), France.

Tumiran was born in Binjai, North Sumatera, Indonesia, on August 23, 1959. He received B.Sc. degree from Department of Electrical Power Engineering, Universitas Gadjah Mada Yogyakarta, Indonesia, in 1985, M.Eng. degree from Department of Electrical Power Engineering, Saitama University, Japan in 1993 and Ph.D degree in Production and Information Sciences, Saitama University, Japan in 1996. He is a Lecturer in the Department of Electrical Engineering and Information Technology, Universitas Gadjah Mada Yogyakarta, Indonesia. His research interests are in power system operation, high voltage engineering, high voltage system insulation, and renewable energy.